Multi-jet ice 3D printing

Pushkar Prakash Kamble, Subodh Chavan, Rajendra Hodgir, Gopal Gote and K.P. Karunakaran
Department of Mechanical Engineering, Indian Institute of Technology Bombay, Mumbai, India

Abstract

Purpose – Multi-jet deposition of the materials is a matured technology used for graphic printing and 3 D printing for a wide range of materials. The multi-jet technology is fine-tuned for liquids with a specific range of viscosity and surface tension. However, the use of multi-jet for low viscosity fluids like water is not very popular. This paper aims to demonstrate the technique, particularly for the water-ice 3 D printing. 3 D printed ice parts can be used as patterns for investment casting, templates for microfluidic channel fabrication, support material for polymer 3 D printing, etc.

Design/methodology/approach – Multi-jet ice 3 D printing is a novel technique for producing ice parts by selective deposition and freezing water layers. The paper confers the design, embodiment and integration of various subsystems of multi-jet ice 3 D printer. The outcomes of the machine trials are reported as case studies with elaborate details.

Findings – The prismatic geometries are realized by ice 3 D printing. The accuracy of 0.1 mm is found in the build direction. The part height tends to increase due to volumetric expansion during the phase change.

Originality/value – The present paper gives a novel architecture of the ice 3 D printer that produces the ice parts with good accuracy. The potential applications of the process are deliberated in this paper.

Keywords 3D printer development, Cryogenic additive manufacturing, Ice 3D printing, Multi-jet 3D printing

Paper type Research paper

1. Introduction

3D printing technology has outgrown its initial application as rapid prototyping. 3 D printing is widely being practiced in various industries such as food, pharma, construction, biomedical devices fabrication, geography, space and manufacturing. 3 D printed food items such as chocolate bars, xanthan gum, gelatin and meats are gaining popularity (Malone and Lipson, 2007; Godoi *et al.*, 2016). 3 D concrete printers help automate the construction process (Paul *et al.*, 2018). 3 D printed drug tablets regulate the rate at which the drug is released (Gibson and Ming, 2001). 3 D printing enables the development of biocompatible and customized tissue scaffolds (Vlasea *et al.*, 2011). Physical models of the terrain are realized from *Geographical Information system (GIS)* data using 3 D printing techniques (Agrawal *et al.*, 2006). As the applications are growing, the 3 D printing technology is being explored for a wide range of non-traditional materials such as glass (Marchelli *et al.*, 2011), wood (Henke and Treml, 2013) and ice (Kamble *et al.*, 2018). Ice is the emerging 3 D printing material, as there are several applications of the ice parts such as investment casting patterns, templates for microfluidic devices fabrication, support structure for photopolymer and 3 D printing. The present article illustrates a multi-jet deposition approach for ice 3 D printing.

Ice 3 D printing produces the ice parts by depositing water layer-by-layer inside an insulated chamber at sub-zero temperature. The pioneering work for the process of ice 3 D printing, termed *Rapid Freeze Prototyping* (RFP), was first done by M C Leu *et al.* in 1991 (Zhang *et al.*, 1999). The model material for RFP is deionized water (melting/freezing point = 0°C), and the support is a saline solution (melting/freezing point = −10°C approx.). The work chamber temperatures are typically −20°C to −25°C (Zhang *et al.*, 1999; Barnett *et al.*, 2009; Zheng *et al.*, 2020).

Inspired by RFP, Pieter Sijpkes in McGill University adopts ice 3 D printing for building architectural models (Barnett *et al.*, 2009; Sijpkes *et al.*, 2009). Jie Jin *et al.* report the use of ice as a highly removable support material for photopolymer 3 D printing, both dispensed through separate dispensers. They use photopolymer as the model material and ice as the support material for the overhanging features (Jin and Chen, 2017). Ice is a beneficial support material as it melts away quickly.

Zheng *et al.* report a single jet ice 3 D printer system that creates the ice micro-scale structures without support (Zheng *et al.*, 2020). Zhang *et al.* report ice 3 D printing for the microfluidic device fabrication applications (Zhang *et al.*, 2015). Humanity is exploring the possibility to create a habitat on Mars. Ice 3 D printing could prove as a house construction strategy due to the availability of ice on Mars, its properties such as thermal insulation and transparency and flexibility of

The current issue and full text archive of this journal is available on Emerald Insight at: **https://www.emerald.com/insight/1355-2546.htm**

Rapid Prototyping Journal
28/6 (2022) 989–1004

[DOI 10.1108/RPJ-03-2021-0065]

Authors gratefully acknowledge the support of Mr. Abhishek Verma, 360 Digital Printing Innovations & the team of Digital Innovations, Indore, India for the present work.

Received 25 March 2021
Revised 2 June 2021
17 September 2021
Accepted 2 December 2021

the 3 D printing process (Morris *et al.*, 2016). The summary of the ice 3 D printing research worldwide is given in Table 1.

Ice 3 D printer comprises the four subsystems, namely, material deposition system, motion system, freezing system and control system. The material deposition system spreads the liquid layer selectively on the work platform. The deposited liquid layer instantly solidifies. Another layer of the liquid is spread selectively on the previous layer and undergoes freezing. The process continues till the frozen object is obtained (Zhang *et al.*, 1999).

Aqueous solutions of various materials such as sodium chloride (NaCl) (Zhang *et al.*, 1999; Barnett *et al.*, 2009), potassium chloride (KCl) (Barnett *et al.*, 2009) and dextrose (Richards *et al.*, 2008) are reported as a support material for overhanging features. The aqueous solutions have a lower melting point (−10 to −15°C) than the model material, i.e. water (0°C). The support material is dispensed wherever the object has some overhanging/undercut features. After printing all layers, the chamber is raised to, say, −5°C, and held at that temperature till the support melts away. Finally, the pure ice part is harvested.

RFP uses a pair of piezoelectric nozzles similar to the extrusion heads in FDM, as shown in Figure 1. A peristaltic pump delivers the water from the reservoir to the nozzle. The motion system maneuvers the nozzle as per the pre-programmed path to reproduce the desired layer geometry. The freezer maintains the temperature of the process at around −20°C. The layer boundary is first printed with a fine nozzle, and then the interior is filled with a larger nozzle. (Zhang *et al.*, 1999).

Although single-jet ice 3 D printers produce good ice parts, there are certain limitations of the single-jet process for ice 3 D printing. The present article encompasses a multi-jet approach in contrast to the single-jet.

2. Key applications of the ice objects

There are several applications of the 3 D printed ice parts. The applications are 3 D visualization, a pattern for investment casting, drug encapsulation, a template for microfluidic channel fabrication and scaffolds for biomedical implants manufacturing. The applications are elaborately subsequently.

2.1 3 D visualization of the object

3D visualization of the computer-aided design (CAD) models is the very first application of the 3 D printing processes. CAD models of the various engineering products can be readily 3 D printed using ice 3 D printing. The ice being a cheaper and sustainable material, it is suitable for the intermediate visualization of the product if only visualization is the purpose. Water can be readily reused without much processing, unlike many other 3 D printing materials. Plastic waste can be avoided. It is easy to make colorful objects of ice by mixing colour pigments with water.

2.2 Patterns for investment casting

As shown in Figure 2, ice parts can be used as the patterns for investment casting (Liu *et al.*, 2002; Zhang and Leu, 2021; Liu *et al.*, 2004; Huang *et al.*, 2004). The ice patterns require the specialized ceramic slurry compositions to work at sub-zero temperatures. It is to ensure the ice patterns do not melt and lose their geometric accuracy.

2.3 Microfluidic devices fabrication

Microfluidic devices are used for pharmaceutical assays. The capillary action of the paper-based microfluidic chips is frequently used to ascertain the controlled flow of the reagents. Polymer-based micro-channels are also used. The fabrication of the microchannels on the polymer requires lengthy procedures to create a silicon wafer template.

Aqueous reagents can be 3 D printed on the cold Peltier cooler surface and frozen and sealed using polymeric encapsulation as shown in Figure 3 (Zhang *et al.*, 2015).

2.4 Support material for various model materials

3D printed ice models are temporary; they leave no trace once they melt; thus, they have exciting applications as a support material/scaffolding for various other 3 D printed materials. Water can be used as a support material for the resin, as shown in Figure 4(a) (Jin and Chen, 2017). The scaffolding structure of the ice can be used in the 3 D printing of the graphene aerogels, as shown in Figure 4(b) (Zhang *et al.*, 2016).

3. Principle of multi-jet ice 3 D printing

A multi-jet print head is a vital part of the multi-jet ice 3 D printing system. The print head comprises a large number of nozzles arranged in multiple rows operated by piezoelectric action.

3.1 Concept of the multi-jet ice 3 D printing process

Figure 5 gives the schematic diagram of the multi-jet ice 3 D printing process. Model material is deionized water (DIW) (freezing/melting point = 0°C), and support material is saline water (freezing/melting point < 0°C, say −15°C). The print head nozzles are divided into two groups that deposit deionized water and saline water separately. However, in the present research, overhanging and undercut-free geometries are discussed where only pure water is deposited to ascertain the jetting of water and prove the feasibility of the process.

3.2 The architecture of the multi-jet ice 3 D printer

The multi-jet 3 D printing system is divided into four subsystems, similar to RFP. The four subsystems are a multi-jet material deposition system maneuvered by the motion system. The workspace is maintained at −20°C to −25°C in an insulated chamber using the refrigeration system (Figure 6). The control system controls the motion and the deposition.

The deposition takes place in the form of droplets generated by the piezoelectric action of the nozzle. Each nozzle has a micro-chamber filled with water where a piezoelectric element is attached to one of the walls (Figure 7). The piezoelectric element expands and contracts in response to the voltage signal. The series of contraction and expansion of the piezoelectric element results in the shockwave, and it ejects the water droplet from the nozzle (Le, 1998).

The authors have developed the prototype of the multi-jet 3 D printing system, as shown in Figure 8. The architectural

Table 1 Worldwide scenario of the ice 3 D printing research

Sl. No.	Institute	Deposition	Material Model	Support	Control	Build strategy	Application	Ref
1	University of Missouri, USA	Single jet, piezoelectric operated nozzle	Water	Aqueous NaCl and dextrose solution	Pulsed voltage signal by a function generator for nozzle and motion control card (AT 600 by CompuMotor) for axes	NC codes for the toolpath, boundary and interior is printed separately	Investment casting	Zhang *et al.* (1999); Liu *et al.* (2002)
2	McGill University, Canada	Single jet, piezoelectric operated nozzle	Water	Aqueous NaCl and KCl solutions	BasicStamp microcontroller to convert the on/off signals for the FDM nozzle to water nozzle with required frequency	NC codes for the toolpath, generated by	Artistic shapes for the architectural purpose	Barnett *et al.* (2009); Sijpkes *et al.* (2009)
3	University of Southern California, USA	Spray-based dispenser system	Resin	Water	Dedicate control system for the deposition and UV curing of the resin layer	Mask-image-projection based stereolithography	Highly removable support for the resin parts	Jin and Chen (2017))
4	Peking University, China	Single jet piezoelectric nozzles	Water	–	ZLAN 6802 controller for motions and piezoelectric deposition control	Voxel-based printing system where each droplet is considered a voxel	Micro-scale ice structures as templates for microfluidic channels	Zheng *et al.* (2020)
5	SEArch (Space Exploration Architecture) and Clouds Arch. Office, USA	Single jet, piezoelectric operated nozzle (in collab. With McGill)	Water	Aqueous NaCl and KCl solutions	Same as #2	Same as #2	Mars ice house, a solution for the construction of habitable house for planet Mars	Morris *et al.* (2016)

Figure 1 Single jet ice 3 D printer

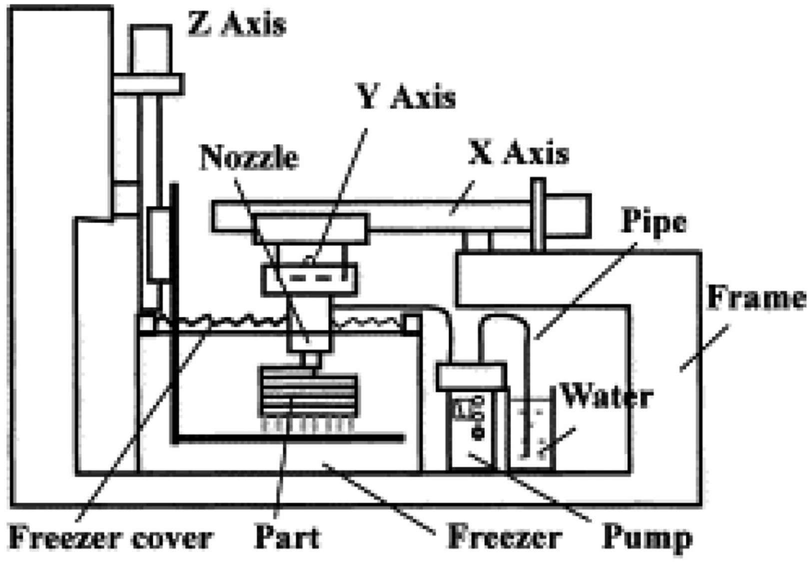

(a)

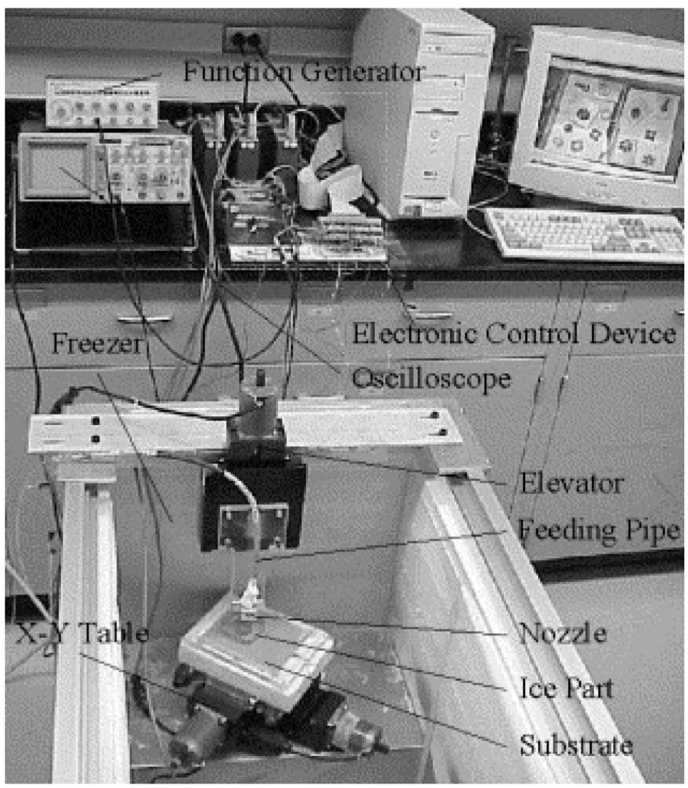

(b)

Notes: (a) Schematic diagram (Zhang *et al.*, 1999); (b) prototype (Liu *et al.*, 2002)

details, the significance of the subsystems, function and the case studies of the 3 D printed ice parts are elaborated subsequently.

3.2.1 Multi-jet deposition system

The multi-jet deposition system comprises the print head, the diaphragm pump, filters, saline and DI water supply tank and buffer tanks. Figure 9 shows the schematic diagram of the multi-jet deposition system, and Figure 10 shows the assembled multi-jet deposition system. Few drops of magenta coloured ink are added to the saline water to identify the printing pattern.

Water supply tank primarily stores and supplies the water to the printhead (Figure 9). A 12 Vdc diaphragm pump with a

Figure 2 Ice parts as the pattern for investment casting)

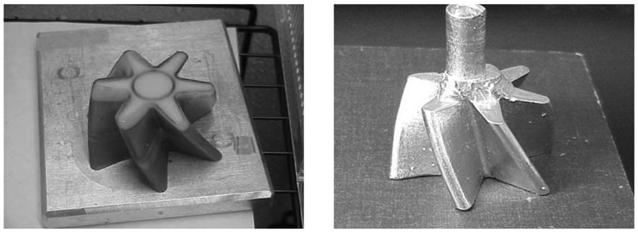

(a) (b)

Notes: (a) 3D printed ice boundary; (b) casting

Source: (Liu *et al.,* 2002)

1.5 m pressure head fills the water supply tank with a maximum flow rate of 0.4 Lmin^{-1}. As shown in Figure 9, the water supply tank has a level sensor. As soon as the supply tank is full, the level sensor cuts off the pump. Water is immediately replenished as soon as the water level in the tank falls, with the help of the level sensor's feedback. Filters of the mesh size 5 micrometer at the diaphragm pump prevent the entry of the particulate matter in the lines. The buffer tanks help in regulating the water supply. Print head deposits the water on the work platform maintained at −25°C. The nozzles of the print head are kept warm using a strip heater to prevent freezing.

The printhead from Xaar plc. is used for the present study (Figure 10). It is a piezoelectric technology-based printhead that has 1280 nozzles arranged in four rows. Figure 11(a) shows the magnified images of the printhead nozzle plate. The nozzles are arranged in four rows in a staggered fashion to cover the maximum area in one pass, as shown in Figure 11(b). The printhead has overall dimensions of 52.7 × 45 × 76.2 mm. The width of the swathe that can be printed in one pass is 27 mm.

The printhead is capable of printing four colours, namely, cyan (C), magenta (M), yellow (Y) and black (K), assigned to the four different rows.

For present prototype, four rows of the printhead are divided into two pairs. The printhead inherently allows rows for black (K) and cyan (C) to be paired and yellow (Y) and magenta (M) to be paired. Y-M pair of nozzle row deposits DI water (model material) and K-C deposits saline water (support material) as shown in Figure 12.

3.2.2 Motion system

The motion system enables the movement of the print head over the work platform in the pre-programmed raster pattern. The print head moves in the ±X and ±Y direction with the stepper/servo motors' help through the belt-driven LM guides, whereas the work platform moves in the ±Z direction with the ball screws driven by stepper/servo motors (Figure 13).

In the present research, NEMA 23 stepper motors are used for all axes. For *x*- and *y*-axes, timing belts are used with T5 pulleys to move the carriage over linear motion guides of 15 mm width. For *z*-axis, a 16-mm diameter ball screw with 5-mm pitch is used. The system works without vibrations with a carriage speed up to 200 mm/s.

3.2.3 Freezing system

The freezing system maintains the workspace at −20° to −25° C. The freezing system comprises the compressor, condenser, evaporator and expansion device (capillary tube), as shown in Figure 14.

The evaporator coils are located in the work envelope. The compressor and condenser units are fitted in the space at the bottom of the frame. Along with a regular refrigeration system, liquid nitrogen is used for the initial cooling of the work chamber.

Figure 3 Microfluidic device fabrication

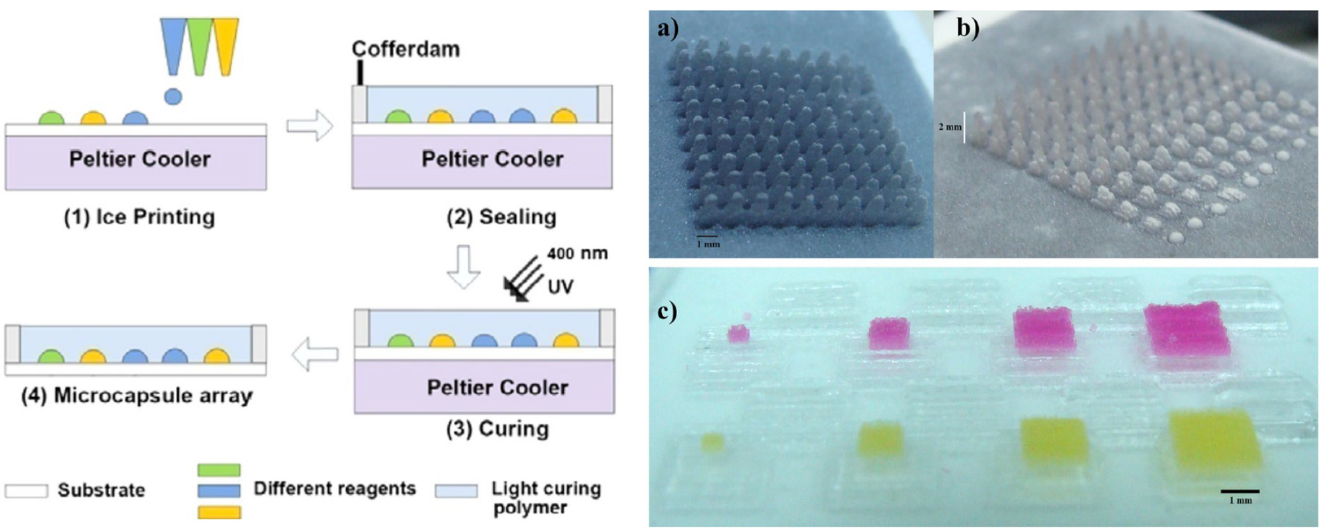

(a) (b)

Notes: (a) Process of microcapsule array fabrication; (b) ice structures for encapsulation

Source: [Reprinted with permission from American Chemical Society Publications, copyright 2015] (Zhang *et al.,* 2015)

Figure 4 Water as a support material

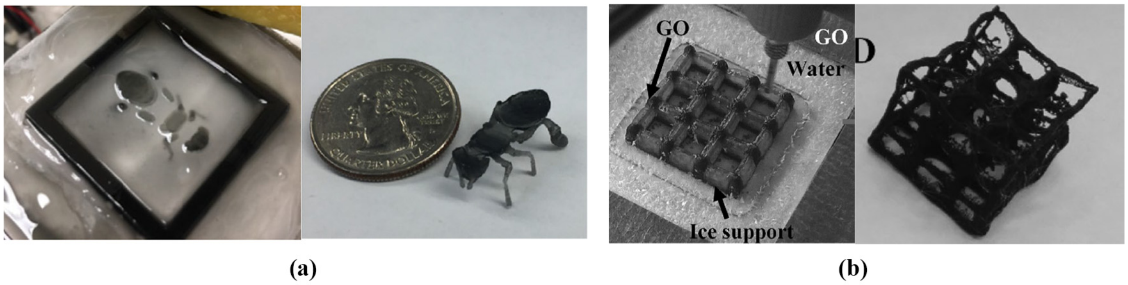

Notes: (a) For resin (Jin and Chen, 2017); (b) for graphene aerogel (Zhang *et al.*, 2016)

3.2.4 Control system
The integrated control system regulates the material deposition system and motion system. The control system carries out the four functions, as explained subsequently.

- Meniscus control
  Water starts to drip from the printhead nozzles under gravity. The meniscus control system maintains a meniscus level at the nozzle. It prevents the accidental dripping of water against the gravity with the vacuum's help (Figure 15). A 12 Vdc, diaphragm type vacuum pump with maximum vacuum capacity of 70 kPa is used to create the vacuum over the tank's water level. A vacuum switch is used to adjust the vacuum as per the desired level. The vacuum switch senses the vacuum in line and gives the feedback to the vacuum pump. The trial and error method is used to find the right vacuum setting for the printhead. It is determined that the vacuum of 2.7 kPa is sufficient to maintain the meniscus of water at the nozzle for the given set up. The air buffer tank prevents the accidental entry of water into the vacuum pump.
- Material deposition control
  The integrated control system controls various parameters related to the material deposition, such as print head speed, frequency of the droplet generation and piezoelectric voltage waveform.
  The voltage waveform decides the jettability of the liquid. The waveform is the pattern of the change in the voltage applied to the piezoelectric element with respect to the time. Change is voltage results in the expansion and contraction of the piezoelectric elements, creating pressure and vacuum changes in the nozzle chamber. Depending on the chamber geometry, multiple expansions and contractions may take place before droplet ejects from the nozzle (fill/fire cycle). After droplet ejection, the position of the piezoelectric element comes back to normal before it gets ready for the next cycle (Zapka, 2018). The waveform used for the present study is shown in Figure 16. A constant voltage of 18 V is applied over the piezoelectric elements. At the start of the voltage pulse, the voltage is slightly reduced to 16.2 V for 1 μs. The piezoelectric elements contract that results in

Figure 5 Multi-jet ice 3 D printing process

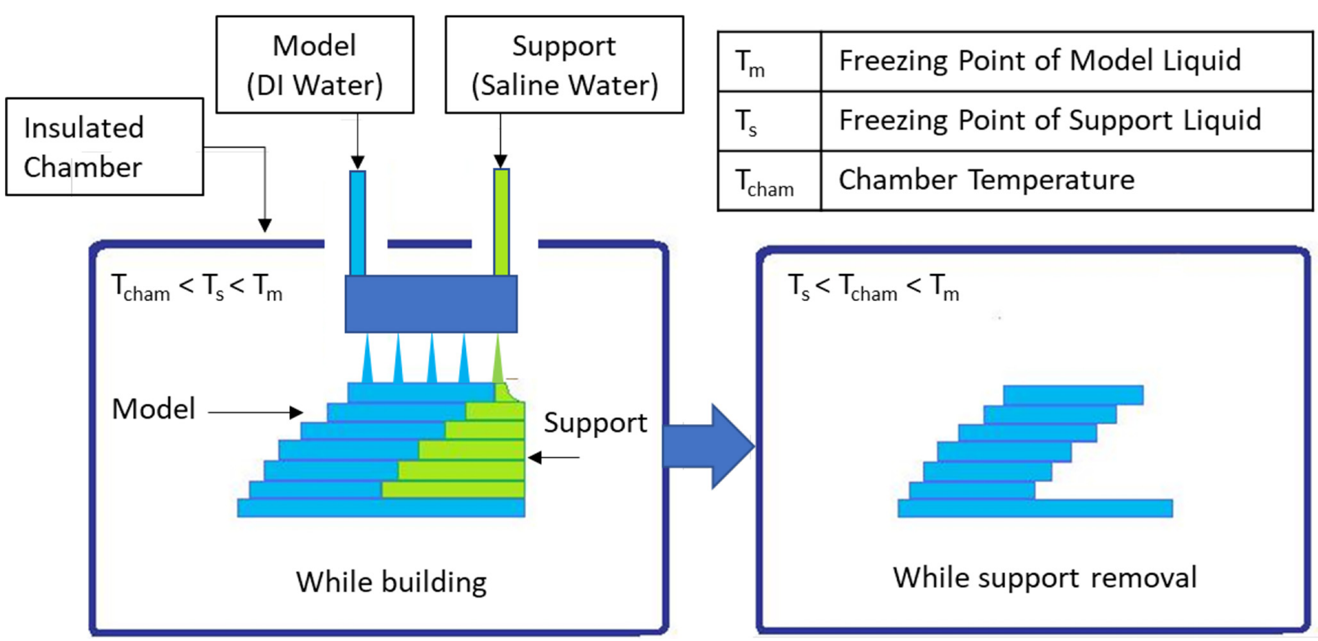

Figure 6 Schematic diagram of the multi-jet 3 D printing system

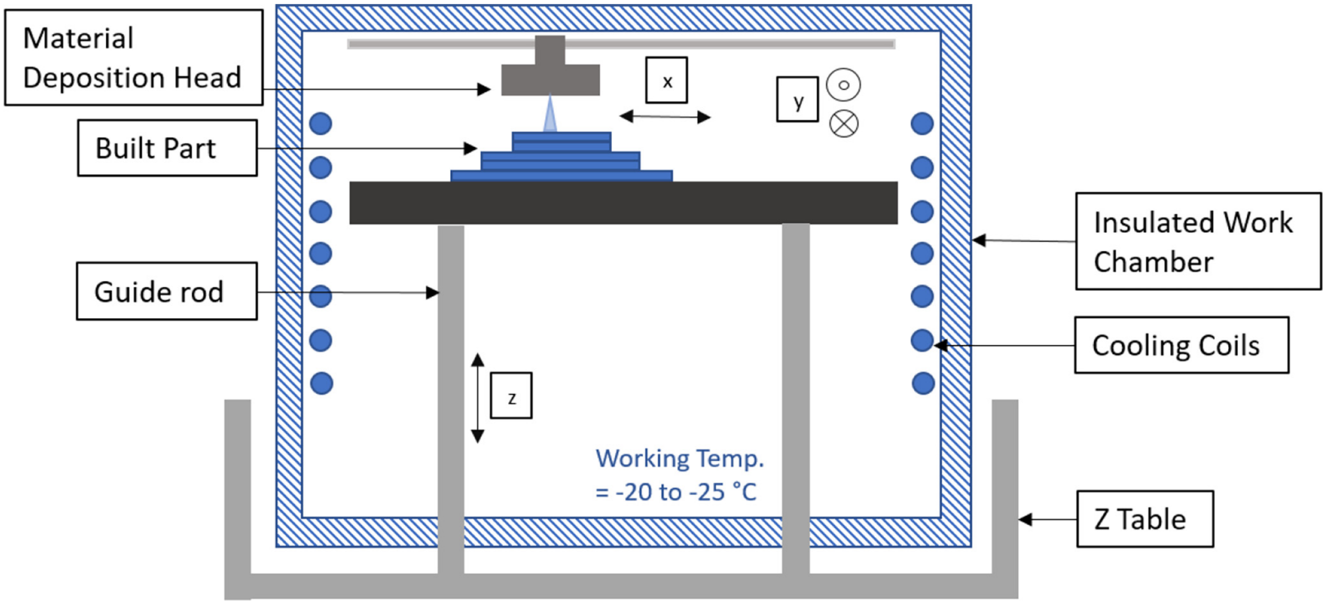

an increase of the chamber volume and water is sucked into the nozzle chamber from the inlet manifold (fill). Voltage is further reduced to 8.64 V and increased to 18 V within 4 μs. It sets the acoustic wave in the chamber. The wave is further reinforced with a quick fall of voltage to 7.2 V and surge to 18 V within 4 μs. The voltage is reduced to 4.14 V within 4 μs and increased to 18.9 V within 2 μs, resulting in an acoustic wave strong enough to eject the droplet out of the chamber (fire). The voltage further normalizes to 18 V within 1 μs. The cycle further continues to eject next droplet. The waveform voltages and time spans are determined and fine-tuned with the several trial and error experiments for the given liquid.

The control circuit for the print head is given in Figure 17. The voltage waveform is fed to the operational amplifier, which applies it to the high side of the piezoelectric element. At any given instant, the voltage is either full or zero, depending on the on-off condition of the nozzle. Each nozzle is turned on by grounding its corresponding MOSFET switch (Apex microtechnology, 2012).

Figure 7 Schematic diagram of a piezoelectric nozzle

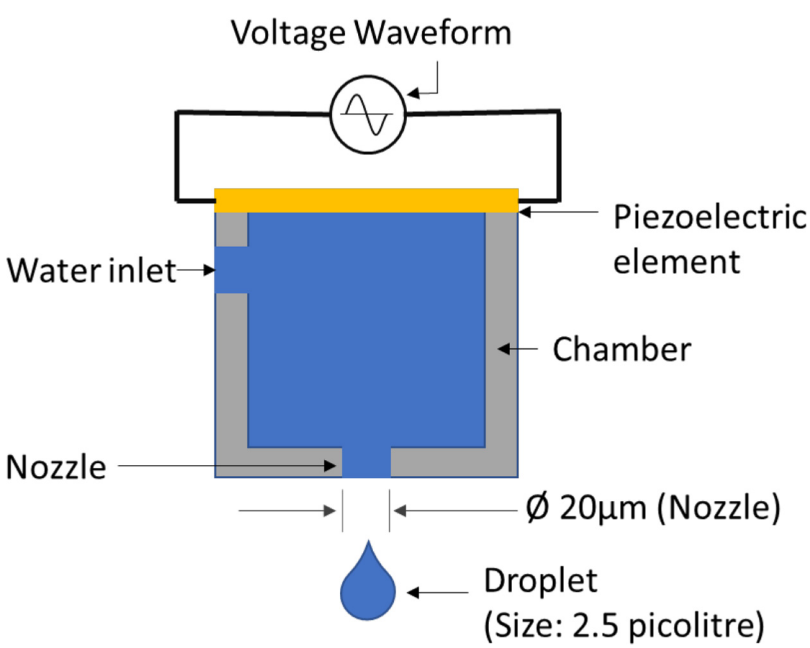

Figure 8 Multi-jet 3 D printer prototype

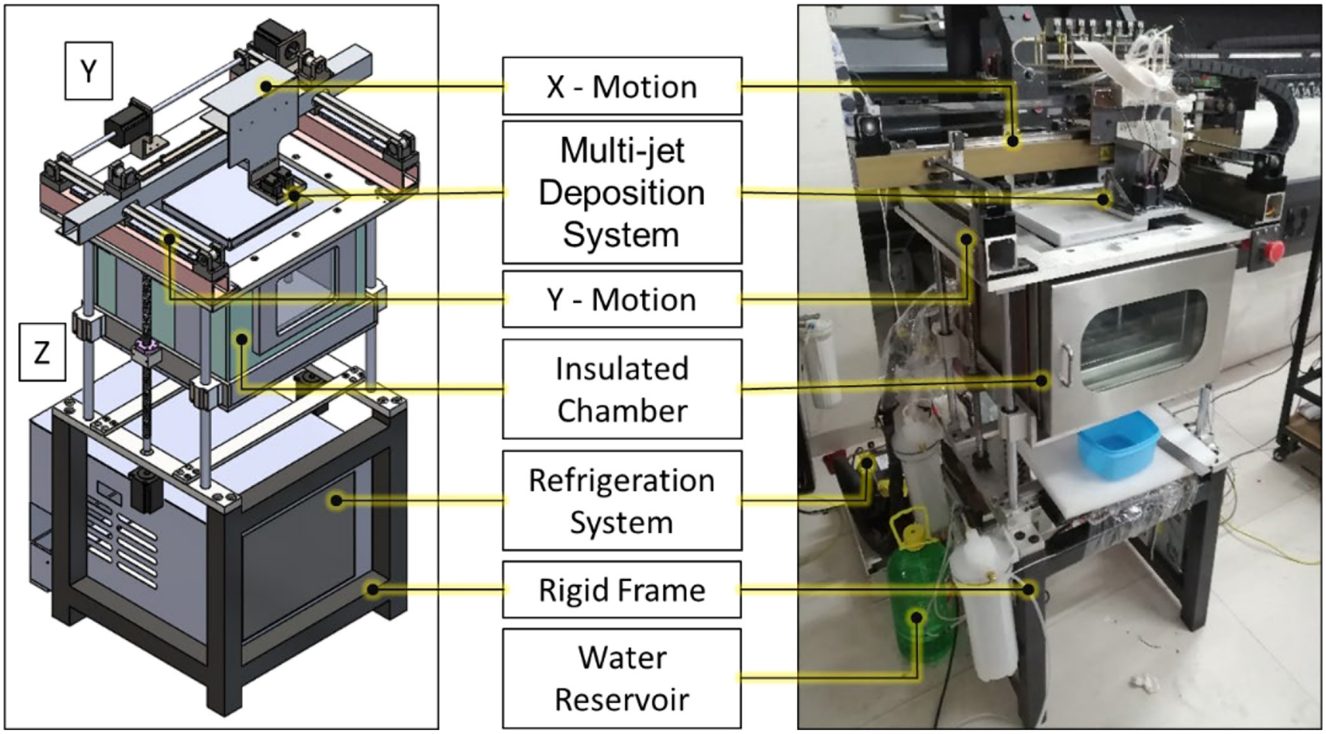

- Motion control
  The motion control involves controlling the stepper/servo motors of the *x*-, *y*- and *z*-axes. The same motors control the print head maneuver speed. The speed is mapped with the droplet generation frequency.
- Print head temperature control
  The print head is maintained at 60°C to protect against the sub-zero temperatures with the help of the two strip heaters of 10 W capacity each (Figure 18). The temperature can be set to a particular point with the help of the integrated control system. For the prototype, the printhead is maintained at 60°C to prevent the freezing of the nozzles.
- A dedicated control system controls the deposition, motion and printhead temperature. The motion and deposition systems are synchronized with the help of the

Figure 9 Schematic diagram of the multi-jet deposition system

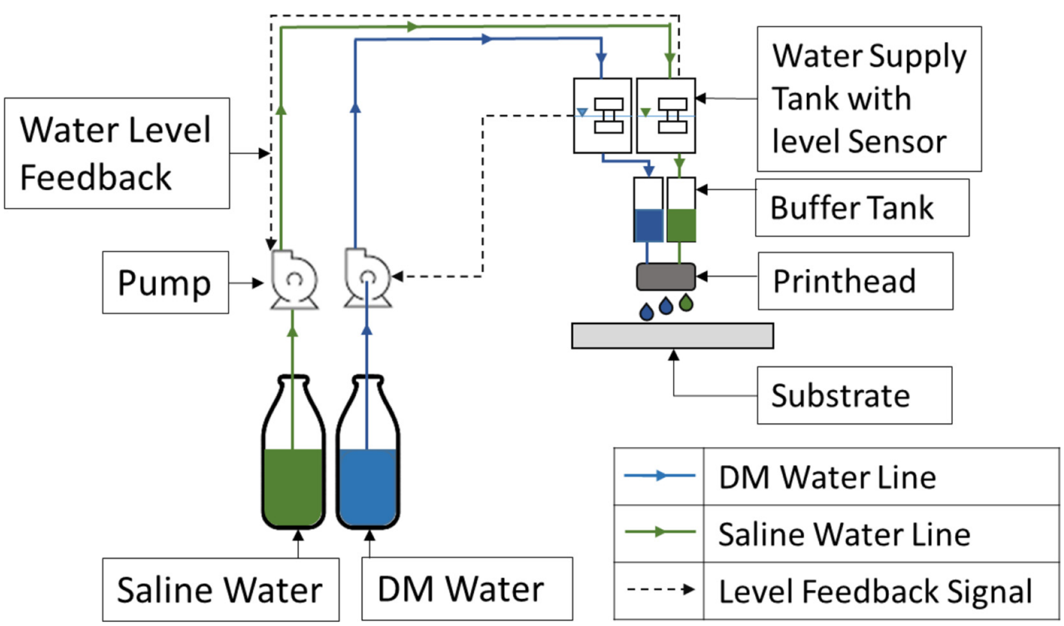

Figure 10 Multi-jet deposition system

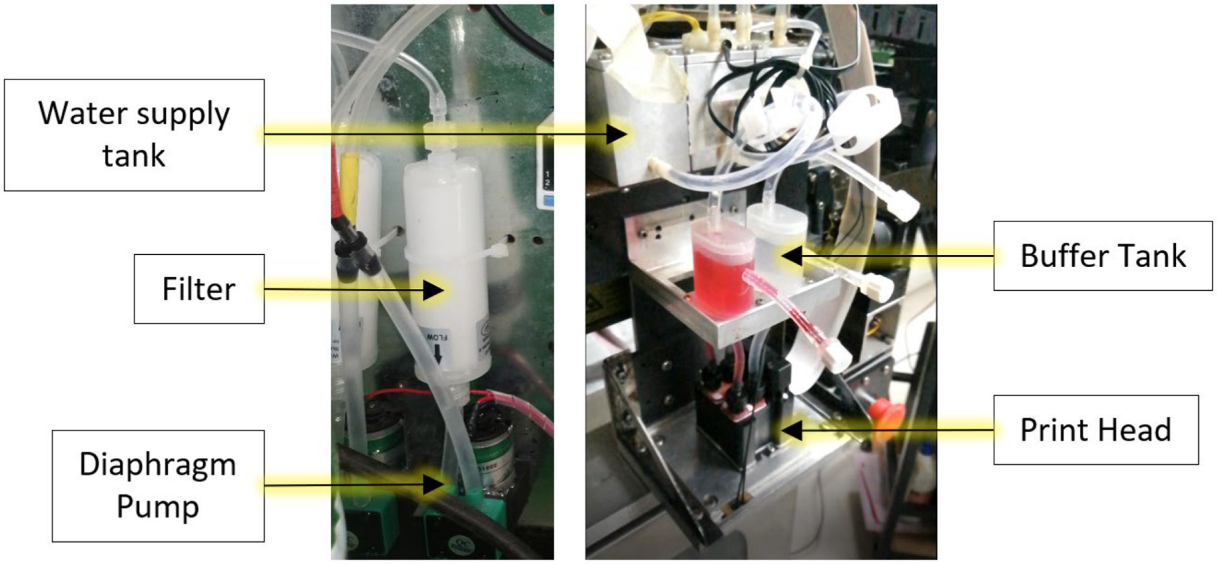

linear encoder. The linear encoder registers the accurate position of the printhead and sends the feedback to the deposition control system. It improves the drop landing accuracy (Table 2).

3.3 Building strategy

As a part of pre-processing, the three-dimensional CAD model in STL file format (Figure 19) is sliced into a series of images in the jpeg format. The jpeg image stores the information of the layer geometry in the form of colour value of each pixel. As a part of the current study, prismatic geometries are used. Each sliced image has the cross-section of the geometry with pixels addressed by dark black colour. *Raster Image Processing (RIP)* is the program that converts the image data to the output specific format (bitmap) for the given printer. Based on the length and width of the output required on the substrate, the image pixels are translated into the data with sequence and distribution of the droplets ejected from the nozzles. This data is stored as a post script file. Post script file is readable for the printhead control hardware. All the sliced images are obtained as a list of post script files. The program sequentially sends the post script files to the printhead that are printed as layers on the substrate to obtain the ice part.

The work chamber is cooled initially with the help of liquid nitrogen. Once the temperature reaches around −20°C, the

Figure 11 Magnified image of the printhead nozzle plate that shows the nozzle diameter and spacing between two nozzles in a row

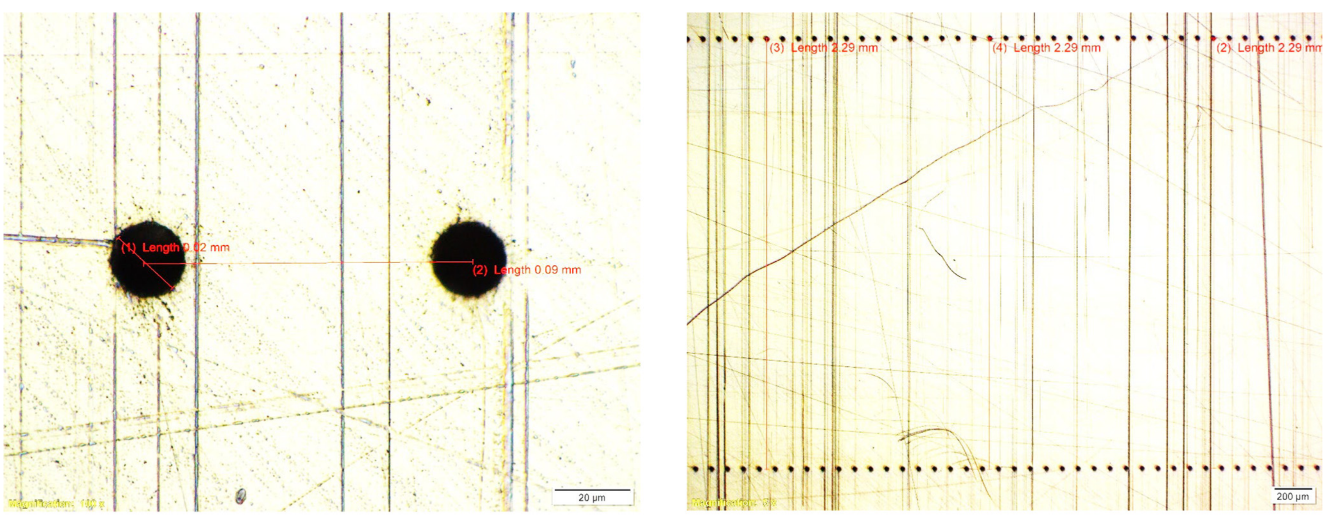

(a) (b)

Notes: (a) Nozzles of the printhead (100x); (b) staggered rows of the nozzles of the printhead (5×)

Figure 12 Division of nozzle rows for model and support materials

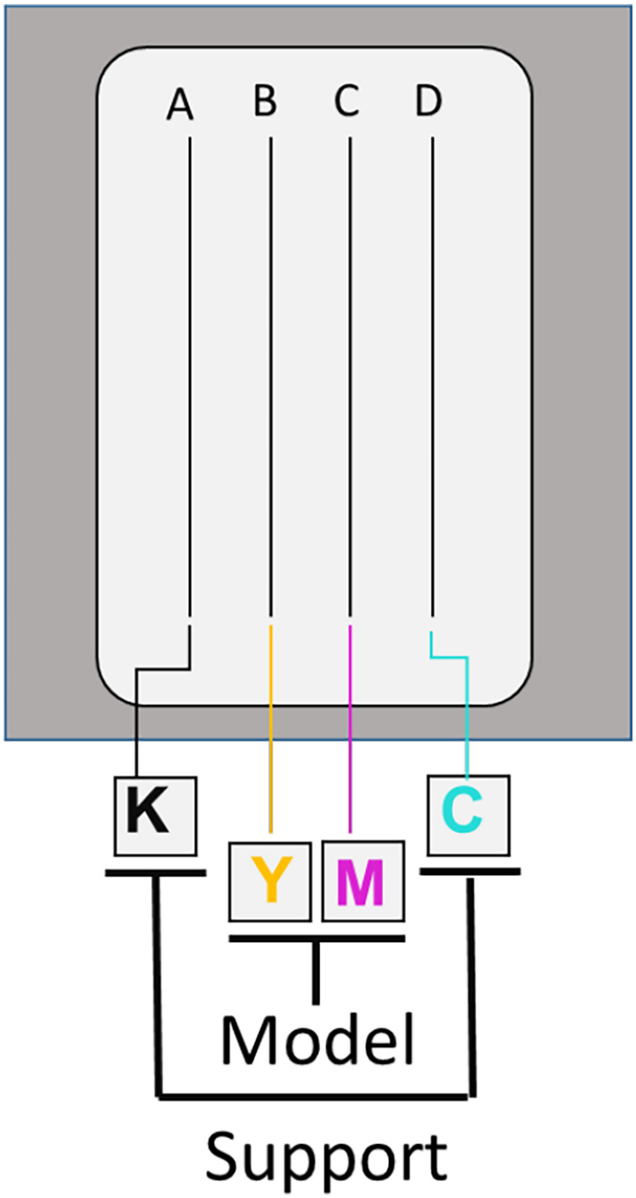

refrigerator starts. The print head is purged at the home location, and the series of images are printed. After the part height reaches 0.5 mm approximately, the worktable is lowered in the Z direction by 0.5 mm. The process of printing continues till all layers are printed.

3.4 Case studies

Two case studies are reported that determine the performance of the system. The prismatic geometries without support material are chosen to prove the concept of the multi-jet ice 3 D printer. In the first case study, as mentioned in Figure 20, the ice model of the acronym of the institute's name (Indian Institute of Technology Bombay – IITB) is printed.

The part height is 5 mm as per the design. The average measured height of the printed part is 5.12 mm (Figure 21).

The visual inspection confirms that the surface is smooth, lustrous and continuous. Phase change takes place for each droplet; thus, the grain structure may not be uniform. The opaque ice model is observed. On the metallic surface, frosting is observed due to the condensation of the moisture. Stair-step effect is observed for the curved surfaces.

In the second case study, the ornamental parts are printed. One is a pendant, and the other is an ornamental piece to be used in the jewelry (Figure 22). The ornamental parts are selected since the ice object's utilization is found in precision casting, such as jewelry. The average measured part height is 5.15 mm.

Figure 23 depicts the layer growth at a microscopic scale. Magnified images show the gradual increase in the height of the ice part.

4. Unique features of the multi-jet ice 3 D printing

The use of multi-jet enables the process of ice 3 D printing to be faster. The multi-jet ice 3 D printing features are predominantly the inherent process capabilities of the multi-jet print head. Table 3 compares the multi-jet technology with the single jet.

- Speed and build strategy

  The deposition takes place by multiple nozzles. The process is faster than the single jet that uses a vector-based toolpath approach (NC codes). In the single jet machines, the boundary is first printed, and then the interior is

Figure 13 Motion system (Rear View)

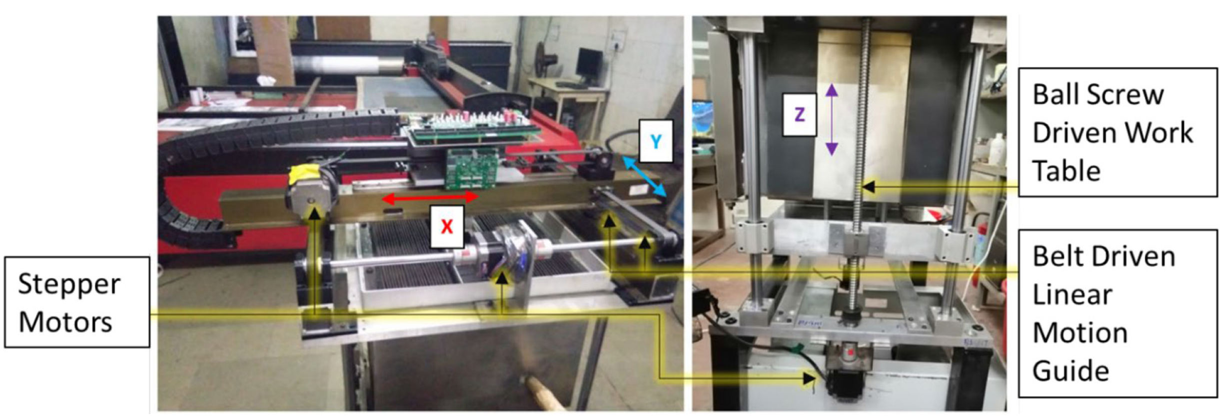

Figure 14 Freezing system

printed, i.e. each point in the layer has to be addressed by the nozzle. In multi-jet printing, the entire layer is printed as a single image without separating the boundary and the interior.

- Resolution and layer thickness
  The resolution of the material deposition determines the accuracy of the printed layer. The resolution of the multi-jet printing is determined as dots per inch (DPI). DPI can be varied to adjust the printing resolution and layer thickness.
- Wide range of materials
  Multi-jet print heads can handle multiple materials concurrently. The multi-jet print head under investigation has four rows of nozzles with 320 nozzles per row. Each row can handle different material. Thus, four different materials can be printed with a single print head.

Figure 15 Schematic diagram of the meniscus control system

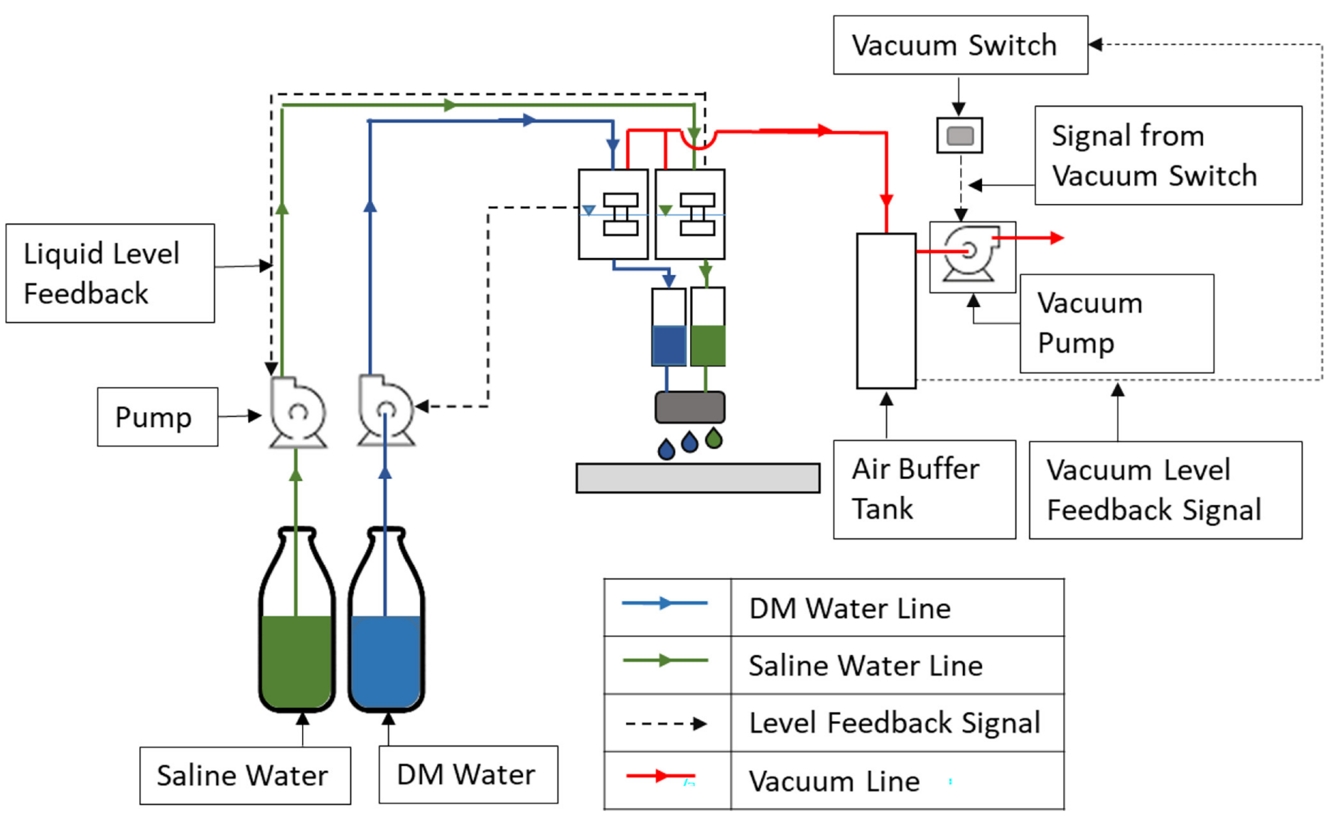

Figure 16 Voltage waveform for the printhead

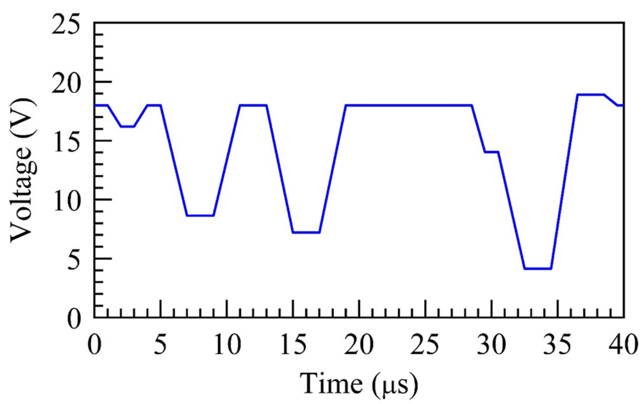

However, in a single jet system, different heads are required to deposit the different materials concurrently. For the proposed system, the four rows are divided into groups of two rows each. One of the groups can deposit model material, and another can deposit the support material.

- Costs

  Machine building cost for the multi-jet machine is marginally more than the single jet system since the multi-jet printhead costs double than the single jet nozzle. However, a multi-jet printhead of 1280 nozzles has a dispensing rate of 10 ml/min (1280 droplets of 2.5 picolitres at the frequency of 50 kHz) as compared to the single jet which has a maximum dispensing rate of 0.9 ml/min (Bryant *et al.*, 2003). Therefore, the productivity of the multi-jet system is 11 times more with higher precision at a marginally higher price. Ice parts can be stored temporality in the 3 D printer itself, or any commonly available freezers. However, the built ice parts are used immediately for the applications as mentioned in Section 2 with minimal storage period; hence, the storage costs incurred will also be minimal.

5. Results and discussion

Water is an abundant and affordable material. 3 D printed ice parts have interesting applications as mentioned in Section 2 despite the need for maintaining a subzero temperature. Multi-jet dispensing technology can produce fast and fine droplets. A multi-jet ice 3 D printer developed as a part of the present study proves the feasibility of the commercial printheads for dispensing water. It is observed that the nozzles work smoothly without freezing as the strip heaters are used to keep the printhead warm.

Case studies show that the accuracy of the parts produced by the multi-jet ice 3 D printing is in the range of +0.1 to +0.2 mm. However, single jet system has the accuracy of +0.6 to +1.9 mm (Liu *et al.*, 2002). The probable reason for a slightly higher accuracy is the smaller droplet size for the multi-jet printhead, resulting in better resolution. Water tends to expand upon freezing due to its anomalous behavior; hence, the object dimensions tend to be slightly greater than expected.

6. Conclusion

Ice parts have several emerging applications in various fields such as investment casting, microfluidic devices fabrication and

Figure 17 Piezoelectric element control circuit

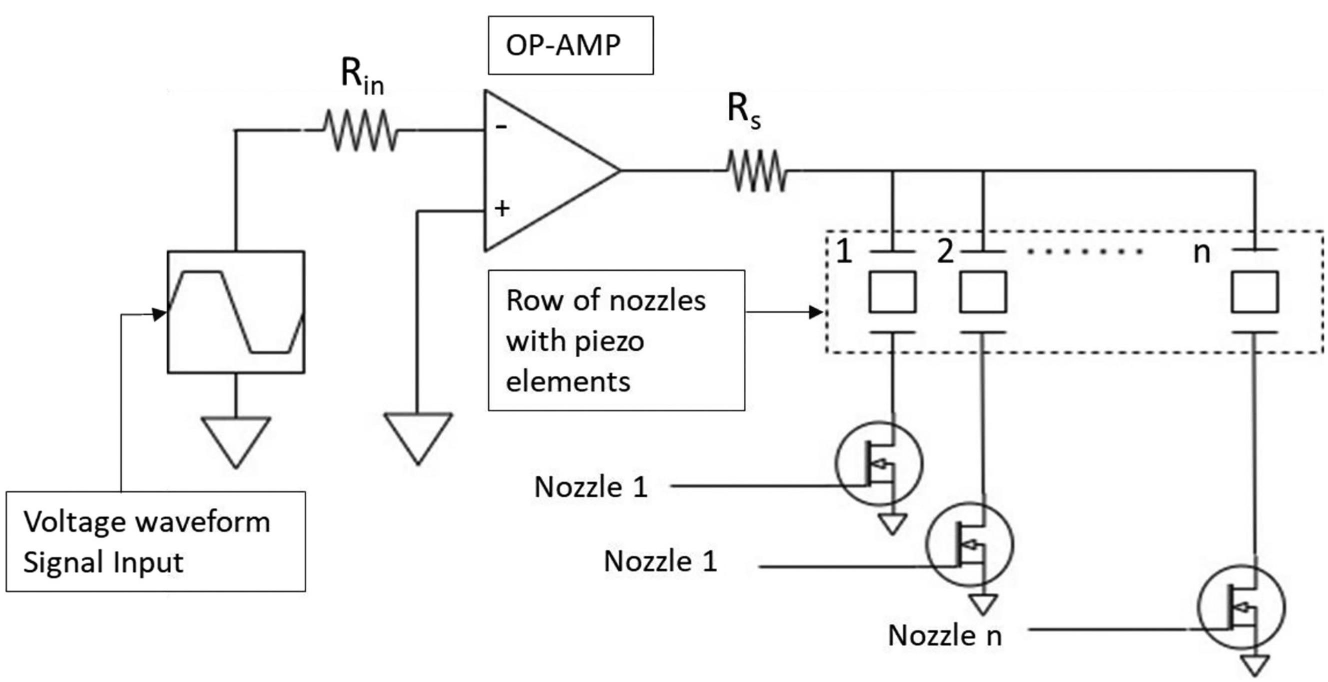

Source: (Apex microtechnology, 2012)

Figure 18 Print head heaters

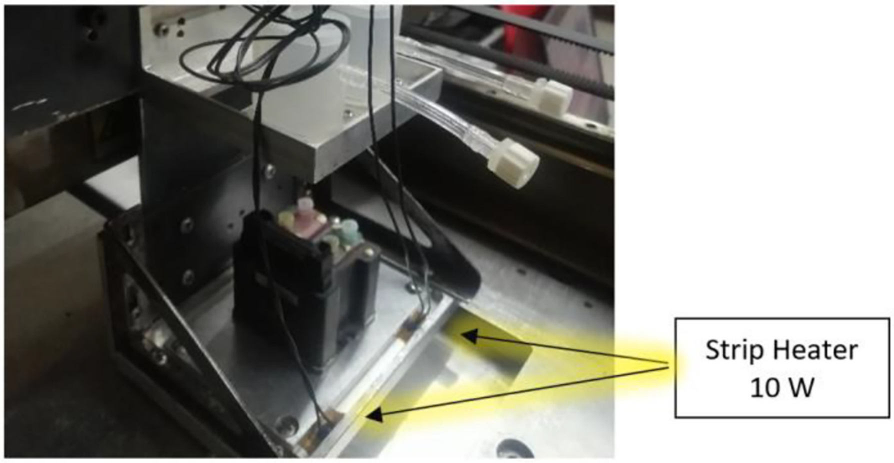

Table 2 Specifications of the multi-jet ice 3 D printer prototype

Sl No.	Specification	Detail
2	Print head	320 nozzles × 4 rows = 1280 nozzles
3	Build volume (L × W × H)	200 × 200 × 150 mm
4	Layer resolution	360 dots per inch
5	Droplet volume	2.5 to 20 picoliter (variable drop size)
6	Layer thickness	0.06 mm
7	Max. deposition speed	200 mm/s
8	Nozzle temperature	60°C
9	Working temperature	−25°C
10	Materials	Water (DIW), Glycerin solution.
11	Connectivity	USB
12	Physical dimensions	970 × 600 × 1300 mm

as a support material in polymer-based 3 D printing processes. 3 D printing is a suitable route to create the parts with desirable geometries. Multi-jet deposition helps meet the challenges in ice 3 D printing, such as precise water deposition, ease of operation and flexible resolution of the layer geometry and layer thickness.

The architecture of the multi-jet ice 3 D printer is presented. The arrangement of the subsystems and their embodiment is unique for low-temperature materials such as ice. The motion system is positioned to minimize the contact with the freezing system inside the working chamber at sub-zero temperature.

Case studies prove the feasibility of the multi-jet technique for low viscosity liquids like water. Multi-jet ice 3 D printing is better than previously reported single jet techniques in several aspects such as speed, build strategy, flexibility and materials.

However, it is also essential to discuss the shortcomings of the technique along with its benefits. The merits and demerits of the multi-jet ice 3 D printing are enlisted below.

6.1 Merits

- The process of multi-jet is faster than the single jet process of deposition. The deposition approach of multi-jet deposition enables a higher resolution and high deposition rate.
- Multiple aqueous solutions can be deposited simultaneously using the print head. Also, the material range is vast since the multi-jet is a robust technology used for various chemicals.

Figure 19 Build process

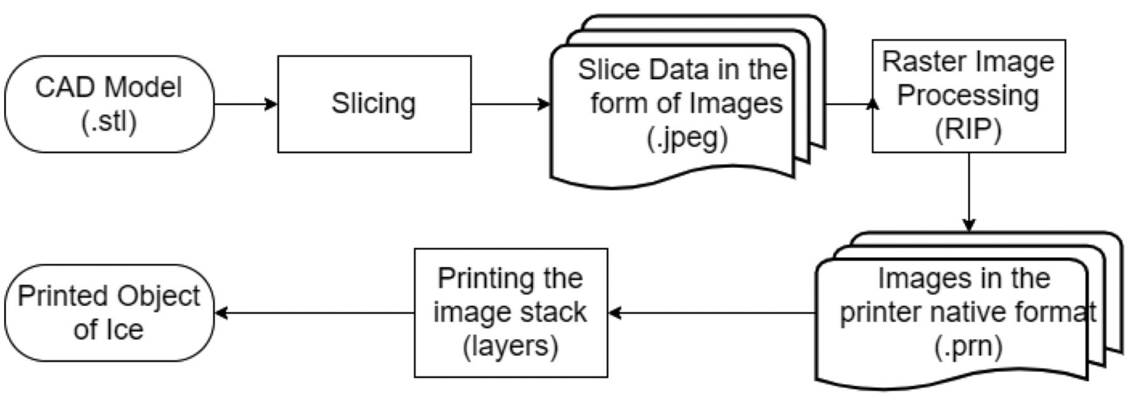

Figure 20 Case study 1: Ice model of the letters of the institute's acronym

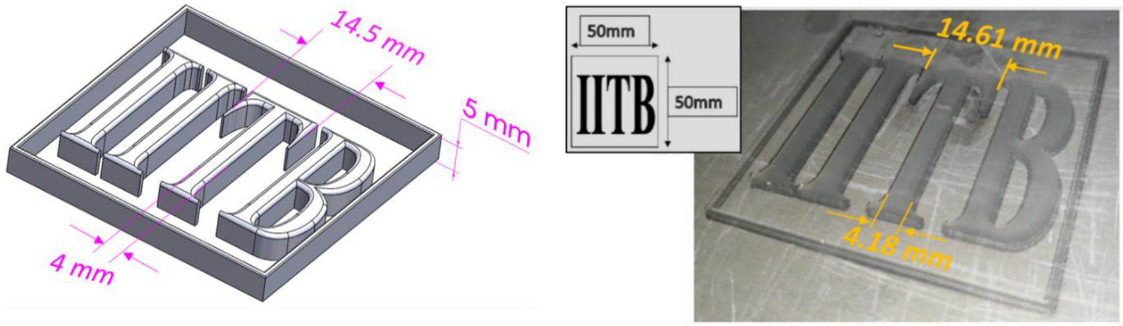

(a) (b)

Notes: (a) CAD model; (b) sliced image and the 3D printed part

Figure 21 Magnified view of the ice model

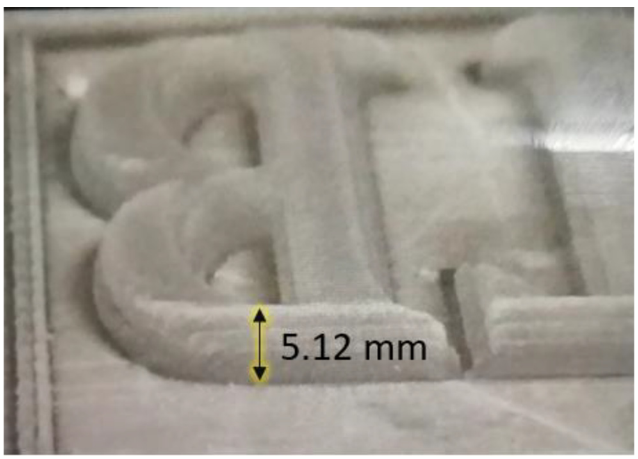

- A novel architecture of the machine protects the motion carrying parts and the electronics from sub-zero temperatures.

6.2 Demerits

- Ice parts have a short life span; thus, there are limitations on their storage and utilization.
- The thermal balance of the system is critical as the lower temperatures can affect the nozzles and freeze the water inside the nozzles; if the nozzle temperature is too high, it can melt the previous layer.
- Multi-jet nozzles need protection from dust or particulate matter. The damage that occurred to the nozzles due to clogging or deposition is irreversible and results in the print head replacement.
- Humidity control is a challenge as the surface of the 3D printed ice part tends to deteriorate with an increase in the

Figure 22 Case study 2: ice model of the ornamental parts

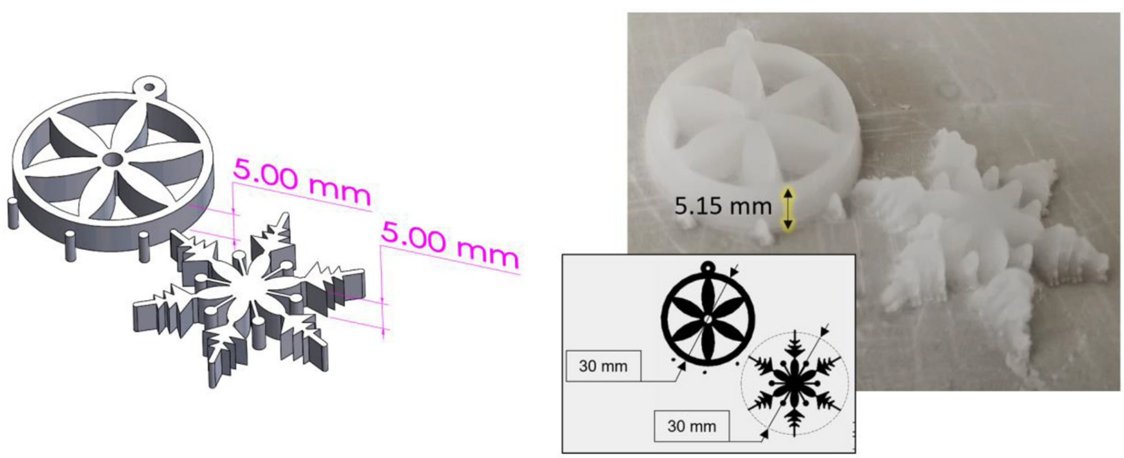

(a) (b)

Notes: (a) CAD model; (b) sliced image and the 3D printed part

Figure 23 Magnified images of the 3 D printed ice layers (Magnification: 60×)

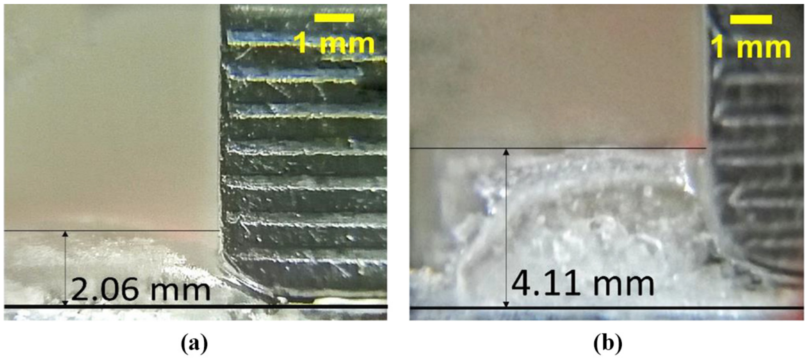

Notes: (a) 35 layers; (b) 70 layers

Table 3 Features of multi-jet ice 3 D printing in comparison with single-jet

Feature	Single-jet	Multi-jet
Number of nozzles	1	1280 (present set up)
Machine input data	NC program	Postscript file
Build strategy	Boundary of the layer is deposited first and then interior is filled as per programmed path	The layer is deposited as a single entity without boundary and interior separation in the preprogramed X-Y raster motion
Time for one layer	High since single nozzle addresses the entire layer	Low as multiple nozzles address the layer
Material	One liquid per printhead	Multiple liquids (up to four for present set up) per print head

humidity by condensation of the atmospheric water vapor on the ice surface and its dendritic growth in the form of ice crystals.

References

Agrawal, S., Antunes, J.P., Theron, E., Truscott, M. and De Beer, D.J. (2006), "Physical modeling of catchment area by rapid prototyping using GIS data", *Rapid Prototyping Journal*, Vol. 12 No. 2, pp. 78-85.

Apex microtechnology (2012), "Driving piezoelectric actuators", Vol. 2012, pp. 1-13.

Barnett, E., Angeles, J. and Pasini, D. (2009), "Robot-Assisted rapid prototyping for ice structures", *IEEE International Conference on Robotics and Automation*, Vol. 33 No. 4, pp. 146-151.

Bryant, F.D., Sui, G. and Leu, M.C. (2003), "A study on effects of process parameters in rapid freeze prototyping", *Rapid Prototyping Journal*, Vol. 9 No. 1, pp. 19-23.

Gibson, I. and Ming, L.W. (2001), "Colour RP", *Rapid Prototyping Journal*, Vol. 7 No. 4, pp. 212-216.

Godoi, F.C., Prakash, S. and Bhandari, B.R. (2016), "3d printing technologies applied for food design: status and prospects", *Journal of Food Engineering*, Vol. 179, pp. 44-54.

Henke, K. and Treml, S. (2013), "Wood based bulk material in 3D printing processes for applications in construction", *European Journal of Wood and Wood Products*, Vol. 71 No. 1, pp. 139-141.

Huang, C., Leu, M.C. and Richards, V.L. (2004), "Investment casting with ice patterns and comparison", *NSF Design and Manufacturing Grantees Conference*, pp. 1-7.

Jin, J. and Chen, Y. (2017), "Highly removable water support for stereolithography", *Journal of Manufacturing Processes*, Vol. 28, pp. 541-549.

Kamble, P. Chavan, S. and Karunakaran, K.P. (2018), "Multi-jet fluid deposition in 3D printing: a review", No. July.

Le, H.P. (1998), "Progress and trends in ink-jet printing technology", *Journal of Imaging Science and Technology*, Vol. 42 No. 1, pp. 49-62.

Liu, Q., Sui, G. and Leu, M.C. (2002), "Experimental study on the ice pattern fabrication for the investment casting by rapid freeze prototyping (RFP)", *Computers in Industry*, Vol. 48 No. 3, pp. 181-197.

Liu, Q., Leu, M.C., Richards, V.L. and Schmitt, S.M. (2004), "Dimensional accuracy and surface roughness of rapid freeze prototyping ice patterns and investment casting metal parts", *The International Journal of Advanced Manufacturing Technology*, Vol. 24 Nos 7/8, pp. 485-495.

Malone, E. and Lipson, H. (2007), "Fab±home: the personal desktop fabricator kit", *Rapid Prototyping Journal*, Vol. 13 No. 4, pp. 245-255.

Marchelli, G., Prabhakar, R., Storti, D. and Ganter, M. (2011), "The guide to glass 3D printing: developments, methods, diagnostics and results", *Rapid Prototyping Journal*, Vol. 17 No. 3, pp. 187-194.

Morris, M., Ciardullo, C., Lents, K., Montes, J., Rudakevych, O., Sono, M., Sono, Y. and Yashar, M. (2016), "Mars ice house: using the physics of phase change in 3D printing a habitat with H2O", *Aiaa Space 2016*, No. July, pp. 673-681.

Paul, S.C., van Zijl, G.P.A.G. and Gibson, I. (2018), "A review of 3D concrete printing systems and materials properties: current status and future research prospects", *Rapid Prototyping Journal*, Vol. 24 No. 4, pp. 784-798.

Richards, V.L., Druschitz, E.A., Isanaka, S.P., Leu, M.C., Cavins, M., Casting, I.I. and Pattern, I. (2008), "Rapid freeze prototyping of investment cast thin-wall metal matrix compostites I – pattern build and molding", The Materials Society Annual Meeting, pp. 143-156.

Sijpkes, P., Barnett, E., Angeles, J. and Pasini, D. (2009), "The architecture of phase change at McGill", *Leadership in Architectural Research*, No. April, p. 241.

Vlasea, M., Shanjani, Y., Basalah, A. and Toyserkani, E. (2011), "Additive manufacturing of scaffolds for tissue engineering of bone and cartilage", *Int. Journal of Advanced Manufacturing Systems*, Vol. 13 No. 1.

Zapka, W. (Ed.) (2018), *Handbook of Industrial Inkjet Printing*, Wiley-VCH.

Zhang, W. and Leu, M.C. (2021), "Investment casting with ice patterns made by rapid freeze prototyping", pp. 66-72.

Zhang, W., Leu, M.C., Ji, Z. and Yan, Y. (1999), "Rapid freezing prototyping with water", *Materials & Design*, Vol. 20 Nos 2/3, pp. 139-145.

Zhang, Q., Zhang, F., Medarametla, S.P., Li, H., Zhou, C. and Lin, D. (2016), "3D printing of graphene aerogels", *Small*, Vol. 12 No. 13, pp. 1702-1708.

Zhang, H.Z., Zhang, F.T., Zhang, X.H., Huang, D., Zhou, Y. L., Li, Z.H. and Zhang, X.X. (2015), "Portable, easy-to-operate, and antifouling microcapsule array chips fabricated by 3D ice printing for visual target detection", *Analytical Chemistry*, Vol. 87 No. 12, pp. 6397-6402.

Zheng, F., Wang, Z., Huang, J. and Li, Z. (2020), "Inkjet printing-based fabrication of microscale 3D ice structures", *Microsystems and Nanoengineering*, Vol. 6 No. 1, available at: https://doi.org/10.1038/s41378-020-00199-x

About the authors

Pushkar Prakash Kamble was born on 13 February 1992 and is presently a PhD student in Rapid Manufacturing Lab at Department of Mechanical engineering, IIT Bombay under the supervision of Prof Karunakaran. He has completed his master's degree from National Institute of Technology, Warangal and bachelor's degree from Sinhgad College of Engineering, affiliated to Pune University. His research interests are multi-jet fluid dispensing, ice 3D printing and CNC. Pushkar Prakash Kamble is the corresponding author and can be contacted at: pushkarkamble@gmail.com

Subodh Chavan was born on 28 November 1994 and is presently working in Rapid Manufacturing Laboratory at Department of Mechanical Engineering, IIT Bombay as a Project Software Engineer under the supervision of Prof. Karunakaran. He has completed his B.Tech and M.Tech from IIT Bombay. His interests are robotics, machine design, control systems, automation and software development.

Rajendra Hodgir is a PhD student in the Mechanical Engineering Department, IIT Bombay. Currently, he is working on additive manufacturing and rapid investment casting, under the guidance of Prof. K. P. Karunakaran. He has completed his M.Tech. from National Institute of Technology, Warangal and B.Tech. from College of Engineering Pune.

Gopal Gote was born on 3 November 1993 and presently he is a PhD student in Rapid Manufacturing Laboratory in the Department of Mechanical Engineering, IIT Bombay, India under the supervision of Prof K P Karunakaran. He completed his M. Tech from NITK Surathkal, India, and B. E. from MGM'S JNEC Aurangabad, India, His area of interest includes foam 3D printing, foam machining, rapid casting, lightweight materials, characterization.

K.P. Karunakran is an institute chair Professor at the IIT Bombay and has been teaching and researching in the areas CNC technology, rapid manufacturing and computer graphics from past 22 years. Prior to this, he worked in Hindustan Aeronautics Limited for about nine years. He was a consultant to Mercedes-Benz Technology Centre in summer 2000 and has been associated with Fraunhofer institutes and TU Dresden since 1998 as a Humboldt Fellow. He has been a Visiting Professor in the University of Metz and Ecole Centrale de Nantes. He developed Magics's "OptiLOM", a pre-processor for LOMRP, in collaboration with DaimlerChrysler and Materialise.